Graphical Abstract (for review)

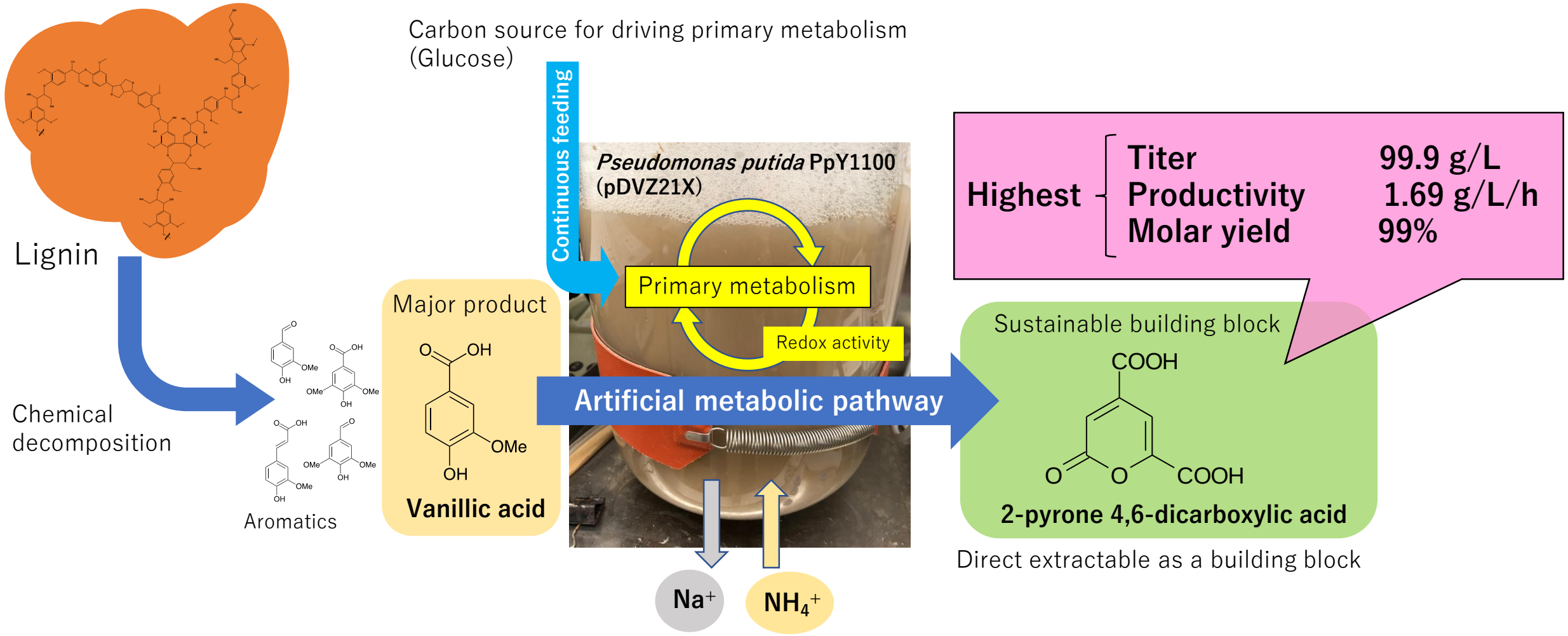

Highlights

Improvement of the production efficiency of PDC from vanillic acid was investigated.

The maintenance of primary metabolic activity is important for PDC production.

Removal of Na ions is important to inhibit PDC-Na complex formation.

PDC production titer reached close to 100 g/L by improved conditions.

High-level production of 2-pyrone-4,6-dicarboxylic acid from vanillic acid as a lignin-related aromatic compound by metabolically engineered fermentation to realize industrial valorization processes of lignin

Yuichiro Otsuka[a,*], Takuma Araki[a], Yuzo Suzuki[a], Masaya Nakamura[a], Naofumi Kamimura[b], Eiji Masai[b]

[a]Department of Forest Resource Chemistry, Forestry and Forest Products Research Institute, Tsukuba, Ibaraki 305-8687, Japan

[b]Department of Materials Science and Bioengineering, Nagaoka University of Technology, Nagaoka, Niigata 940-2188, Japan

* Corresponding author: Yuichiro Otsuka

Department of Forest Resource Chemistry, Forestry and Forest Products Research Institute, Matsunosato 1, Tsukuba, Ibaraki 305-8687, Japan

E-mail address: yotuka@ffpri.affrc.go.jp

Phone: +81-29-829-8282

ABSTRACT

2-pyrone-4,6-dicarboxylic acid (PDC) is a valuable building block molecule produced from lignin-derived aromatic compounds by biological funneling. This study aimed to design a fermentation process for producing PDC from vanillic acid, which could be applied at an industrial production. Metabolomic analysis revealed that a high primary metabolic activity within cells was required to improve the production efficiency. Moreover, a medium with ammonium salts and no alkali metals was advantageous because it suppressed the formation of PDC–metal complexes. Our optimized process yielded the highest PDC titer and productivity ever reported: 99.9 g/L and 1.69 g/L/h, respectively. Per batch, 190 g of PDC was produced per liter of initial culture media, and the final liquid volume was 1.9 L. Our study demonstrates the design of fermentation processes for the advanced industrial utilization of lignin by biological funneling. (136 words)

Key words

Lignin, 2-Pyrone 4,6-dicarboxylic acid, Biological funneling, Vanillic acid, Industrial production

1. Introduction

Fossil resources can be replaced to achieve a circular economy by producing raw materials for bio-based polymers through the microbial fermentation of renewable resources. Building blocks such as lactic acid, succinic acid, and polyhydroxyalkanoic acid can be produced by the microbial fermentation of monosaccharides obtained by the enzymatic saccharification of lignocellulosic biomass (Kawaguchi et al., 2016). Lignin, constituting 9–34% of lignocellulosic biomass, is the second most abundant renewable resource on earth after cellulose (Phaiboonsilpa et al., 2010; Rabemanolontsoa & Saka, 2013; Ragauskas et al., 2014). However, its complex and heterogeneous structure precludes its effective use as a resource.

Previously, a novel technique was proposed to convert aromatic monomers, obtained by chemical degradation of lignin, into a single building block – 2-pyrone-4,6-dicarboxylic acid (PDC) – using microbial metabolism (Otsuka et al., 2006). Recently gaining attention under the name "biological funneling" (Beckham et al., 2016), this method has been used to obtain *cis,cis*-muconic acid, polyhydroxyalkanoic acids, and PDC from aromatic compounds of low-molecular weight derived from the oxidative degradation of lignin (Weiland et al., 2022).

PDC is a pseudoaromatic compound with two carboxy groups on the pyrone ring. Chemical synthesis of this unique molecular structure is difficult, leaving microbial fermentation as the only option for its production. PDC is expected to have new properties unprecedented in petroleum-based chemicals. Polyesters, polyamides, and polyurethanes based on PDC possess excellent mechanical and adhesive properties, besides being biodegradable (Cheng et al., 2022; Hasegawa et al., 2009; Hishida et al., 2009; Michinobu et al., 2010; Michinobu et al., 2009; Michinobu et al., 2011; Shikinaka et al., 2013).

Sphingobium sp. strain SYK-6 is the most enzymatically and genetically studied bacteria for

metabolizing lignin-derived aromatic compounds via the protocatechuic acid (PCA) 4,5-cleavage pathway (Kamimura et al., 2017; Masai et al., 2007), wherein PDC is produced as an intermediate. Therefore, several PDC production systems use metabolic genes from SYK-6 (Johnson et al., 2019; Lee et al., 2022; Otsuka et al., 2006; Suzuki et al., 2020; Suzuki et al., 2022; Yun Qian, 2016).

The major low-molecular weight compounds formed during the oxidative degradation of lignin include the aromatic carboxylic acids vanillic acid (VA), syringic acid, and *p*-hydroxybenzoic acid, and the aromatic aldehydes vanillin, syringaldehyde, and *p*-hydroxybenzaldehyde (Schutyser et al., 2018). In addition, alkaline treatment of grass biomass yields the low-molecular weight aromatics ferulic acid and *p*-coumaric acid (Suzuki et al., 2022). Although processes have been developed to produce PDC from these compounds (Johnson et al., 2019; Lee et al., 2022; Perez et al., 2019; Perez et al., 2022; Suzuki et al., 2020; Suzuki et al., 2021; Yun Qian, 2016), their low efficiency makes them unsuitable for industrial application. A highly efficient PDC production method that can be used in an industrial production is lacking.

Polylactic acid, the most commercialized bio-based polymer, is produced from lactic acid, which is obtained by microbial fermentation of sugars. The first target value for the lactic acid production process was 100 g/L (Abdel-Rahman et al., 2013), and several systems with yields surpassing 200 g/L have already been reported (Tsuge et al., 2019). In the case of metabolites like lactic acid, the target metabolite and energy, both, can be obtained simultaneously through the production metabolic pathway, allowing high-density production with a simple fermentation process. On the other hand, since PDC is produced through an artificial metabolic pathway that does not utilize the glycolytic system, separately metabolizing carbon sources for energy is necessary. This complex fermentation process is one of the major factors responsible for the low productivity of PDC. The highest PDC yield reported to date is 58 g/L (molar yield of 80.7% and productivity of 0.2 g/L/h) from *p*-

hydroxybenzoic acid (Johnson et al., 2019). PDC cannot compete with fossil resource-based plastics if its production efficiencies do not exceed 100 g/L.

This study aimed to design a PDC production process having an efficiency of 100 g/L, despite employing separate pathways for metabolite and energy production. VA was chosen as the substrate, and glucose (Glc) was chosen as the carbon source to drive energy metabolism. This paper reports PDC yields close to 100 g/L, achieved by improving the composition of medium and fermentation process based on metabolomic analysis.

2.Materials and Methods

2.1. Bacterial strains, plasmids, media, and chemicals

The host strain (*Pseudomonas putida* PpY1100) and plasmid (pDVZ21X) used in this study have been described previously (Suzuki et al., 2022). The lysogeny broth (LB) medium (10 g/L Bacto Tryptone, 5 g/L yeast extract, 5 g/L NaCl) was used as the nutrient medium. The Wx medium was used as the inorganic salt medium (Araki et al., 2020). Cultures were grown in L-shaped test tubes at 30°C and shaken at 160 rpm. If necessary, 12.5 mg/L nalidixic acid and 25 or 50 mg/L kanamycin (Km) were added to the medium. All commercially available chemicals except PDC were purchased from Sigma-Aldrich Japan (Tokyo, Japan) and Wako Pure Chemical Industries, Ltd. (Osaka, Japan). PDC was prepared according to a previous method and its purity and structure were verified (Otsuka et al., 2006).

2.2. Fed-batch fermentation

2.2.1 Strain preparation and culture conditions

The PpY1100 strain harboring pDVZ21X was grown in 10 mL of LB medium containing 50 mg/L Km for 12–15 h. The resulting cultures were incubated in 10 mL of pre-culture medium (1.8% (w/v) Glc, 5.6 g/L $(NH_4)_2SO_4$, 3.6 g/L KH_2PO_4, 8.2 g/L Na_2HPO_4, 4.2 g/L yeast extract, 1% (v/v) metal solution including 10.75 g/L MgO, 2.00 g/L $CaCO_3$, 4.50 g/L $FeSO_4 \cdot 7H_2O$, 1.44 g/L $ZnSO_4 \cdot 7H_2O$, 1.12 g/L $MnSO_4 \cdot 4H_2O$, 0.25 g/L $CuSO_4 \cdot 5H_2O$, 0.28 g/L $CoSO_4 \cdot 5H_2O$, 0.06 g/L H_3BO_3, and 5.13% (v/v) 12 N HCl) at a final concentration of 1% (v/v) for 12–15 h. The bacterial cells were washed two times and resuspended in the same medium as before. Cell density was estimated using a spectrophotometer (V-630BIO; JASCO Co., Ltd., Tokyo, Japan) by measuring the optical density at 660 nm (OD_{660}). The recipes of the main culture media were as follows: Na-medium I (1.8% (w/v)

Glc, 6.0 g/L $(NH_4)_2SO_4$, 3.9 g/L KH_2PO_4, 22.2 g/L $Na_2HPO_4 \cdot 12H_2O$, 1.5 g/L yeast extract, 1% (v/v) metal solution); Na-medium II (3.6% (w/v) Glc, 6.0 g/L $(NH_4)_2SO_4$, 3.9 g/L KH_2PO_4, 22.2 g/L $Na_2HPO_4 \cdot 12H_2O$, 2.9 g/L yeast extract, 2% (v/v) metal solution); NH_3-medium (3.6% (w/v) Glc, 6.7 g/L $(NH_4)_2SO_4$, 4.3 g/L KH_2PO_4, 9.1 g/L $(NH_4)_2HPO_4$, 6.5 g/L yeast extract, 8% (v/v) metal solution).

2.2.2. Cultivation and feeding control

Cell suspensions were inoculated at an OD_{660} of 0.001 into a 5-L jar (BMS-10NP3, ABLE Co., Tokyo, Japan) containing 1 L of main culture medium with 25 mg/L of Km. Cultures were operated at 28°C, with an aeration rate of 3.5 vessel volumes per minute, and an agitation speed of 700 rpm. To maintain the medium pH at 6.5, 5 N NaOH was used for Na-medium I and Na-medium II, and 14% (w/v) ammonia solution was used for NH_3-medium. H_3PO_4 (2 M) was used for all media. When the oxygen saturation dropped below 20%, the stirring speed was manually increased up to 1000 rpm. Antifoam A Concentrate (Sigma-Aldrich Japan) was added to defoam when bubbles were formed.

When the OD_{660} of the culture reached 6–8, 610 mg/mL of Glc solution was fed at a flow rate of 7.8 mL/h using a peristaltic pump. When the OD_{660} reached 40–50, the Glc solution was stopped and a mixed solution of 230 mg/mL Glc and 220 mg/mL VA was fed at a flow rate of 21 mL/h. The feeding rates of VA and Glc were 4.8 g/h throughout the culture. Samples were periodically collected and analyzed for cell proliferation (OD_{660}) and various metabolites. Two independent experiments are indicated as solid and dashed lines in Fig. 1C. The error bars show the standard deviation of the both replicates in Fig. 6.

2.3. Metabolomic analysis

The volume of samples required for metabolomic analysis was determined according to the following formula:

Sampling volume (mL) = $20/OD_{600}$

Bacterial cells were collected from the samples by paper filtration. The filter paper was subsequently dipped into 2 mL of methanol containing the internal standard, and the cells were completely suspended by sonication for 30 s, collected in tubes that were sealed with caps, and stored at −80°C.

The bacterial cell suspension was centrifuged at 2,300×g, 4°C for 5 min after 1,600 µL of chloroform and 640 µL of ultrapure water were added to it. The aqueous phase was then centrifuged at 9,100×g, 4°C for 120 min using ultrafiltration tubes with a 5-kDa cutoff (Ultrafree-MC UFC3LCC; Merck Millipore, Burlington, MA, USA). The resulting filtrate was dried and dissolved in 50 µL of ultrapure water.

Metabolomic analysis and characterization was outsourced to Human Metabolome Technology. A combination of capillary electrophoresis (CE) and time-of-flight mass spectrometry (MS) was used for analysis. Sheath liquid, standards for time-of-flight correction, and internal standards were all prepared using Human Metabolome Technology metabolomics kits. Standard mixtures for annotating and quantifying metabolites were prepared using 403 commercially available compounds. The pump, G1603A CE-MS adapter kit, and G1607A CE-ESI-MS sprayer kit were purchased from Agilent Technologies Inc (Santa Clara, CA, USA). The sheath flow rate was adjusted to 10 µL/min. The separation of the metabolites was carried out using a fused silica capillary (50-µm inner diameter × 80-cm total length; Polymicro Technologies, Inc., Phoenix, AZ, USA) with 50 mM ammonium acetate (pH 8.5) for the anion analysis and 1 M formic acid for the cation analysis. The voltage

applied to the CE has been set at 30 kV. The MS spectra were sampled between m/z 50 and 1000. The time-of-flight MS acquisition rate was set to 1.5 spectra/s. MS was performed in the negative ionization mode at 3500 V for anion analysis and 4000 V for cation analysis.

The data processing was carried out using MasterHands™, which was developed by the Institute for Advanced Biosciences at Keio University. The retention time correction for internal standards and authentic substances was applied to each peak of CE-MS. Presumed metabolites were identified from their *m*/*z* and corrected retention times obtained from standard mixtures were analyzed under the same CE conditions. Tolerances were ±10 ppm for *m*/*z* and ± 0.5 min for migration time correction. After manually confirming these results, the peak area of each metabolite was normalised to the corresponding internal standard peak area. MasterHands™ was used for statistical analysis of the remaining metabolites.

2.4. Analytical methods

Supernatants were collected from culture samples by centrifugation, diluted 100–1,000-fold with mobile phase solvent (10% acetonitrile containing 10 mM phosphoric acid), filtered through a 0.45-μm syringe filter with a nylon membrane, and injected into a C-18 Inertsil ODS-3 reverse-phase column (4.6 × 250 mm, 5-μm column; GL Sciences Inc.) to detect VA, PCA, and PDC using an ultraviolet–visible detector set at 290 nm. The analyses were performed isocratically at 40°C with a flowrate of 1 mL/min. The concentration of each compound was calculated by comparing the obtained peak areas with the calibration curves prepared for the compound samples. Glc concentration in the medium was assayed by a combination of mutase and Glc oxidase using the Glucose CII Test kit (Wako Pure Chemical Industries, Ltd., Osaka, Japan).

3. Results and discussion

3.1. Engineering a *P. putida* PpY1100 recombinant for producing PDC from VA

To engineer a pathway to produce PDC from VA, the VA *O*-demethylase gene (*vanAB*) of *P. putida* KT2440 and the PCA 4,5-cleavage pathway genes of *Sphingobium* sp. SYK-6 – PCA 4,5-dioxygenase (*ligAB*) and 4-carboxy-2-hydroxymuconate-6-semialdehyde dehydrogenase (*ligC*) – were introduced into a broad-host-range vector pKT230MC to obtain the plasmid pDVZ21X (Suzuki et al., 2022). In this plasmid, *vanA*, *vanB*, *ligA*, *ligB*, and *ligC* are transcribed as an operon under the control of the *lac* promoter, and are non-inducibly expressed at a high level. pDVZ21X was then introduced into *P. putida* PpY1100 to obtain a recombinant that can produce PDC from VA (Fig. 1A).

3.2. Metabolomic analysis during PDC fermentation with stepwise Glc feeding

A previous study reported PDC titers of more than 10 g/L from PCA using a PpY1100 strain harboring *ligAB* and *ligC*, indicating that a high bacterial cell density at the start of PCA feeding is important for efficient PDC production (Otsuka et al., 2006). Accordingly, the culture conditions were designed for PpY1100 (pDVZ21X) using VA as a substrate (Fig. 1B). PpY1100 (pDVZ21X), pre-cultured in LB, was inoculated into Na-medium I containing 18 g/L Glc and incubated until the culture reached the late log phase (P3 in Fig.1B). Then, Glc was added at once to a final concentration of 50 g/L that is almost double of final feed weight of VA, and the continuous feeding of VA was initiated simultaneously. The PDC concentration reached 21.8 g/L after 17 h of VA feeding (27 h of incubation) (Fig. 1B). However, VA accumulated in the culture after 12 h of VA feeding (22 h of incubation) (Fig. 1B), whereas PCA did not, suggesting that VanAB activity is

bottlenecked in this production pathway (Fig. 1B). Glc was consumed steadily in the early stages, but its consumption became moderate after 22 h of incubation, when VA began to accumulate (Fig. 1B). After the addition of Glc, the cell density increased and settled down to a steady state (Fig. 1B).

In the VA demethylation reaction mediated by VanAB, the reduced form of nicotinamide adenine dinucleotide (NADH), used as a cofactor, is oxidized to NAD^+ (Fig. 1B), which in turn serves as a cofactor for oxidative reactions in central metabolism like the tricarboxylic acid (TCA) cycle, eventually getting reduced back to NADH. An intracellular redox imbalance might underlie the accumulation of VA in the late stages of fermentation. To understand the intracellular state of PpY1100 (pDVZ21X) during fermentation, metabolite dynamics were investigated by metabolomics. Figure 2 shows the quantitative results of primary metabolites obtained through metabolomics. Glycolysis, the pentose phosphate pathway, and the TCA cycle were all activated when Glc was added in the late log growth phase (P3 in Fig. 2). Simultaneously, the levels of energy carriers, such as NAD, NAD phosphate, ATP, and ADP, were also increased, suggesting high intracellular metabolic activity. However, the accumulation of pyruvic acid was observed at P4 in Fig.2. This result may indicate a stagnation of glycolytic metabolites due to the addition of large amounts of glucose at once. This stagnation of the glycolytic system may be related to the growth of the bacteria shifted to a stagnant phase from P3 to P4. On the other hand, when VA began to accumulate, the concentrations of compounds involved in the TCA cycle increased (P5 in Fig. 2), accompanied by a significant decrease in the levels of each amino acid and energy carrier (P5 and P6 in Fig. 2). These results suggest that VA accumulates due to reduced primary metabolic activity. Therefore, to effectively produce PDC from VA, cells must be maintained at a high primary metabolic activity.

3.3. Enhancing PDC productivity by continuous Glc feeding and additional metabolomic

analysis

To improve the production efficiency of PDC from VA, Glc was fed continuously instead of stepwise to maintain a high primary metabolic activity within PpY1100 (pDVZ21X) cells.

These modifications resulted in PDC titers reaching 33 g/L with an extended log growth phase (Fig. 1C). In addition, VA did not accumulate in the fermentation culture, indicating that maintaining a high primary metabolic activity during PDC production is important for maintaining VanAB activity.

Figure 3 shows the results of metabolomic analysis at points P1–P6 in Fig. 1C. During the growth phase (P1–P2) and just after initiating the continuous feed of Glc and VA (P3), primary metabolites remained at high levels, suggesting that PpY1100 (pDVZ21X) was metabolically active. In the early stage of PDC conversion (P4), the level of primary metabolites decreased, but was maintained constant due to the addition of glucose. In the late stage (P5–P6), however, primary metabolites depleted despite continuous Glc addition, indicating that the metabolic activity of PpY1100 (pDVZ21X) had diminished in the late fermentation stage, and that components besides the carbon source also need to be supplemented.

3.4. Additional augmentation of fermentation media and precipitation of insoluble PDC–metal complexes

Based on the above results, the Na-medium II, which contains double the amount of initial Glc, yeast extract, and metal solution compared with Na-medium I, was designed to further improve PDC productivity.

The continuous feed of VA and Glc was started 14 h after incubating PpY1100 (pDVZ21X). Resultantly, the cell density increased until 38.5 h of incubation, and the PDC titer reached 26.4 g/L

(Fig. 4). Thereafter, the cell density slightly decreased, but the PDC concentration continued to increase, finally reaching 73.4 g/L after 159 h of incubation (Fig. 4).

In addition to Glc, increased amounts of yeast extract and metal solution significantly increased cell density and improved the maximum value of OD_{660} from about 35 to 80 compared to the previous experiment (Fig. 1C and Fig. 4). In Fig. 1C, the logarithmic growth phase shifted to a stationary phase after 24 hours. In Fig. 4, the logarithmic growth phase was extended up to 40 hours. These results indicate that the reinforcement of the carbon source as well as other components has enabled further cell growth. The increase in cell density then leads to an increase in the PDC production capacity in the fermenter. As a result, the production of PDC at 40 hours of incubation in both Fig. 1C and Fig. 4 is almost equal to 30 g/L, but in Fig. 4, the VA to PDC conversion activity was maintained afterwards, and the final production efficiency of 73.4 g/L was achieved.

To synthesize PDC-based polymers, purifying the produced PDC from the fermentation media is essential. Therefore, a method of extracting PDC from cultures wherein it had accumulated to high concentrations was investigated. When fermented media was acidified using concentrated HCl, a white precipitate formed corresponding to the PDC–Na complex, whose structure has already been determined (Michinobu et al., 2007) (Fig. 5). PDC is known to chelate alkali metal ions at certain concentrations (Bito et al., 2017; Shikinaka et al., 2018). Na-medium II contains Na^+ ions, and NaOH was used to prepare VA solution and adjust the pH of the medium. Therefore, the formation of PDC–Na complexes is highly likely and Na^+ ions in the medium were considered responsible for the formation of insoluble white precipitates during PDC purification.

3.5. Replacing Na salt in fermentation media with ammonium salt to suppress PDC–metal complexes improved PDC productivity

Ion exchange is necessary to circumvent the formation of PDC–Na complexes, which hinder PDC's utility as a building block. Thus, the NH_3-medium, wherein all Na salts from Na-medium II were replaced with ammonium salts was designed. In addition, ammonia solution was used to prepare the VA solution and adjust the medium pH instead of using NaOH. Furthermore, as the target value of 100 g/L had not yet been reached in the experiment with Na-medium II, the amount of yeast extract and metal solution was further increased in the NH_3-medium. The results of PDC fermentation in NH_3-medium are shown in Fig. 6. The growth of PpY1100 (pDVZ21X) was comparable to that in Na-medium II. The continuous feed of VA and Glc was initiated when the OD_{660} of the culture reached 40–50. After 53 h of fermentation, the PDC concentration reached 96.7 g/L, showing a higher production efficiency than the previous batches. However, 1.07 g/L of VA had accumulated at this point. Therefore, the supply of VA was stopped and only Glc was fed, resulting in the conversion of the accumulated VA to PDC, which increased its titer to 99.9 g/L with a molar yield of 99% after 59 h of fermentation (Fig. 6).

Acidifying the fermentation media did not yield any PDC-derived insoluble salts (Fig. 5) and PDC could be purified by liquid–liquid extraction using ethyl acetate. Gomez et al. reported that PDC spontaneously reacts with ammonium ions to form pyridine 2,4-carboxylic acid (PDCA) at conditions above pH 7.5 (Gomez-Alvarez et al., 2022). In PDC production experiments with NH_3-medium, no PDCA production was observed, although the concentration of ammonium ions was increased by addition of ammonia solution, because the pH was controlled at 6.5.

In summary, NH_3-medium not only enables the purification of directly usable PDC but also improves PDC productivity, probably because ammonium salts, being a nitrogen source, enhance cell metabolism, besides inhibiting the formation of chelator complexes.

The target of 100 g/L for industrial production of PDC from VA was almost achieved. Despite the

different final PDC production efficiencies, the maximum value of OD_{660} is around 70-80 in both experiments with Na-medium II (Fig.4) and NH_3-medium (Fig.6), even the amount of yeast extract and metal solution are further increased in NH_3-medium. This is considered to be the physical upper limit of cell density in the present experimental system. Thereafter, cell density decreases, but cell activity is maintained, suggesting that conversion of VA to PDC continues in the experiment with NH_3-medium. At a later stage of PDC fermentation, accumulation of Glc was observed at the same time as VA started to accumulate. These results suggest that a decrease in cellular activity causes a decrease in VA to PDC conversion activity. And under current conditions, it would probably be difficult to sustain the PDC conversion activity any longer.

To further improve the titer, the problem of VA solubility needs to be solved. Since the solubility of VA in ammonia solution is about 220 g/L, the increase in volume of the fermentation media due to the addition of VA and Glc solutions leads to the dilution of PDC: a trade-off for the higher PDC titer. To solve this problem, the direct addition of VA in powder form was examined but it significantly and immediately decreased cell density and completely suppressed the conversion activity (data not shown). Therefore, a method of adding feedstock that does not significantly increase the volume of the fermentation media must be explored. The other major component, aldehyde-type vanillin, is also obtained through chemical decomposition of lignin, but its solubility is even lower than VA (about 140 g/L).

Finally, 99.9 g/L of PDC could be produced from VA with a productivity of 1.69 g/L/h (molar yield of 99%) by optimizing the medium components and fermentation conditions based on metabolomic analysis. Per batch, 190 g of PDC per 1.9 L of final medium was produced, despite starting with 1 L of culture medium. NH_3-medium also inhibits the formation of PDC–Na complexes, enabling the easy purification of PDC by liquid–liquid extraction. Since this process does

not require a subsequent ion exchange step, the cost of purifying PDC is expected to reduce compared with its proposed recovery by precipitation of PDC–Na complexes (Perez et al., 2022).

This technique is costlier than any general fermentation method like lactic acid fermentation because it requires another carbon source to drive primary metabolism, besides the substrate. For a more practical process, replacing carbon sources with cheaper ones, such as inedible sugar, could also be considered. Sonoki et al. have developed a glucose-free production process, wherein some compounds from the lignin-derived aromatic mixture are used as feedstock for the product while others are used as a carbon source (Sonoki et al., 2018). This strategy could also be applied to the PDC production process. In addition, to produce PDC with a high titer from lignin-derived aromatics, a method for adding substrates without increasing the volume of the fermentation media would be advantageous, besides maintaining the primary metabolic activity of the fermenting microorganisms.

4. Conclusions

This study used metabolomic analysis to optimize the medium composition and fermentation process for producing PDC from VA, a major product of the oxidative decomposition of lignin. Replacing all sodium salts in the medium with ammonium salts suppressed the formation of PDC–Na complexes, maintained cell metabolism by providing a nitrogen source, and improved the production efficiency of PDC as a directly usable building block. Finally, this study achieved the highest PDC titer of 99.9 g/L and productivity of 1.69 g/L/h to date.

CRediT authorship contribution statement

Yuichiro Otsuka: Methodology, Validation, Investigation, Formal analysis, Writing – original draft, Writing – review & editing, Visualization, Supervision, Project administration, Funding acquisition. Takuma Araki: Methodology, Validation, Investigation, Resources, Writing – review & editing, Visualization. Yuzo Suzuki: Methodology, Investigation, Resources, Writing – review & editing. Masaya Nakamura: Methodology, Investigation, Writing – review & editing. Naofumi Kamimura: Resources, Investigation, Writing – review & editing. Eiji Masai: Resources, Investigation, Writing – review & editing.

Declaration of Competing Interest

The authors declare that they have no known competing financial interests or personal relationships that could appear to have influenced the work reported in this paper.

Data availability

Data will be made available on request.

Acknowledgements

We would like to thank Dr Yoshihiro Katayama, Professor Emeritus of the Tokyo University of Agriculture and Technology, for his helpful discussions. This research was supported by a grant from the Forestry and Forest Products Research Institute. We deeply grateful Ms. Rie Iimura for her help with quantitative analysis by HPLC.

References

Uncategorized References

1. Abdel-Rahman, M.A., Tashiro, Y., Sonomoto, K. 2013. Recent advances in lactic acid production by microbial fermentation processes. *Biotechnol Adv*, **31**(6), 877-902.
2. Araki, T., Tanatani, K., Kamimura, N., Otsuka, Y., Yamaguchi, M., Nakamura, M., Masai, E. 2020. The Syringate O-Demethylase Gene of Sphingobium sp. Strain SYK-6 Is Regulated by DesX, while Other Vanillate and Syringate Catabolism Genes Are Regulated by DesR. *Appl Environ Microbiol*, **86**(22).
3. Beckham, G.T., Johnson, C.W., Karp, E.M., Salvachua, D., Vardon, D.R. 2016. Opportunities and challenges in biological lignin valorization. *Curr Opin Biotechnol*, **42**, 40-53.
4. Bito, M., Otsuka, Y., Nakamura, M., Masai, E., Katayama, Y., Shigehara, K., Shikinaka, K. 2017. Unique Complexation Behavior of Alkali Metal Ions and 2-Pyrone-4,6-Dicarboxylic Acid (PDC) Obtained from a Metabolic Intermediate of Lignin. *Waste and Biomass Valorization*. **10,** 1261-1265.
5. Cheng, Y., Kuboyama, K., Akasaka, S., Araki, T., Masai, E., Nakamura, M., Michinobu, T. 2022. Polyurethanes based on lignin-derived metabolic intermediate with strong adhesion to metals. *Polymer Chemistry*, **13**(48), 6589-6598.
6. Gomez-Alvarez, H., Iturbe, P., Rivero-Buceta, V., Mines, P., Bugg, T.D.H., Nogales, J., Diaz, E. 2022. Bioconversion of lignin-derived aromatics into the building block pyridine 2,4-dicarboxylic acid by engineering recombinant Pseudomonas putida strains. *Bioresour Technol*, **346**, 126638.
7. Hasegawa, Y., Shikinaka, K., Katayama, Y., Kajita, S., Masai, E., Nakamura, M., Otsuka, Y., Ohara, S., Shigehara, K. 2009. Tenacious Epoxy Adhesives Prepared from Lignin-derived Stable Metabolic Intermediate. *Sen'i Gakkaishi*, **65**(12), 359-362.
8. Hishida, M., Shikinaka, K., Katayama, Y., Kajita, S., Masai, E., Nakamura, M., Otsuka, Y., Ohara, S., Shigehara, K. 2009. Polyesters of 2-Pyrone-4,6-dicarboxylic Acid (PDC) as Bio-based Plastics Exhibiting Strong Adhering Properties. *Polymer Journal*, **41**(4), 297-302.
9. Johnson, C.W., Salvachúa, D., Rorrer, N.A., Black, B.A., Vardon, D.R., St. John, P.C., Cleveland, N.S., Dominick, G., Elmore, J.R., Grundl, N., Khanna, P., Martinez, C.R., Michener, W.E., Peterson, D.J., Ramirez, K.J., Singh, P., VanderWall, T.A., Wilson, A.N., Yi, X., Biddy, M.J., Bomble, Y.J., Guss, A.M., Beckham, G.T. 2019. Innovative Chemicals and Materials from Bacterial Aromatic Catabolic Pathways. *Joule*, **3**(6), 1523-1537.
10. Kamimura, N., Takahashi, K., Mori, K., Araki, T., Fujita, M., Higuchi, Y., Masai, E. 2017. Bacterial

catabolism of lignin-derived aromatics: New findings in a recent decade: Update on bacterial lignin catabolism. *Environ Microbiol Rep*, **9**(6), 679-705.
11. Kawaguchi, H., Hasunuma, T., Ogino, C., Kondo, A. 2016. Bioprocessing of bio-based chemicals produced from lignocellulosic feedstocks. *Curr Opin Biotechnol.* **42**, 30-39.
12. Lee, S., Jung, Y.J., Park, S.J., Ryu, M.H., Kim, J.E., Song, H.M., Kang, K.H., Song, B.K., Sung, B.H., Kim, Y.H., Kim, H.T., Joo, J.C. 2022. Microbial production of 2-pyrone-4,6-dicarboxylic acid from lignin derivatives in an engineered Pseudomonas putida and its application for the synthesis of bio-based polyester. *Bioresour Technol*, **352**, 127106.
13. Masai, E., Katayama, Y., Fukuda, M. 2007. Genetic and biochemical investigations on bacterial catabolic pathways for lignin-derived aromatic compounds. *Biosci Biotechnol Biochem*, **71**(1), 1-15.
14. Michinobu, T., Bito, M., Tanimura, M., Katayama, Y., Masai, E., Nakamura, M., Otsuka, Y., Ohara, S., Shigehara, K. 2010. Synthesis and Characterization of Hybrid Biopolymers of L-lactic Acid and 2-Pyrone-4,6-dicarboxylic Acid. *Journal of Macromolecular Science, Part A*, **47**(6), 564-570.
15. Michinobu, T., Bito, M., Yamada, Y., Katayama, Y., Noguchi, K., Masai, E., Nakamura, M., Ohara, S., Shigehara, K. 2007. Molecular Properties of 2-Pyrone-4,6-dicarboxylic Acid (PDC) as a Stable Metabolic Intermediate of Lignin Isolated by Fractional Precipitation with Na+Ion. *Bulletin of the Chemical Society of Japan*, **80**(12), 2436-2442.
16. Michinobu, T., Bito, M., Yamada, Y., Tanimura, M., Katayama, Y., Masai, E., Nakamura, M., Otsuka, Y., Ohara, S., Shigehara, K. 2009. Fusible, Elastic, and Biodegradable Polyesters of 2-Pyrone-4,6-Dicarboxylic Acid (PDC). *Polymer Journal*, **41**(12), 1111-1116.
17. Michinobu, T., Hiraki, K., Inazawa, Y., Katayama, Y., Masai, E., Nakamura, M., Ohara, S., Shigehara, K. 2011. Click synthesis and adhesive properties of novel biomass-based polymers from lignin-derived stable metabolic intermediate. *Polymer Journal*, **43**(7), 648-653.
18. Otsuka, Y., Nakamura, M., Shigehara, K., Sugimura, K., Masai, E., Ohara, S., Katayama, Y. 2006. Efficient production of 2-pyrone 4,6-dicarboxylic acid as a novel polymer-based material from protocatechuate by microbial function. *Appl Microbiol Biotechnol*, **71**(5), 608-14.
19. Perez, J.M., Kontur, W.S., Alherech, M., Coplien, J., Karlen, S.D., Stahl, S.S., Donohue, T.J., Noguera, D.R. 2019. Funneling aromatic products of chemically depolymerized lignin into 2-pyrone-4-6-dicarboxylic acid with Novosphingobium aromaticivorans. *Green Chemistry*, **21**(6), 1340-1350.
20. Perez, J.M., Sener, C., Misra, S., Umana, G.E., Coplien, J., Haak, D., Li, Y., Maravelias, C.T., Karlen, S.D., Ralph, J., Donohue, T.J., Noguera, D.R. 2022. Integrating lignin depolymerization with microbial funneling processes using agronomically relevant feedstocks. *Green Chemistry*, **24**(7), 2795-2811.
21. Phaiboonsilpa, N., Yamauchi, K., Lu, X., Saka, S. 2010. Two-step hydrolysis of Japanese cedar as treated by semi-flow hot-compressed water. *Journal of Wood Science*, **56**(4), 331-338.
22. Rabemanolontsoa, H., Saka, S. 2013. Comparative study on chemical composition of various biomass species. *RSC Advances*, **3**(12).
23. Ragauskas, A.J., Beckham, G.T., Biddy, M.J., Chandra, R., Chen, F., Davis, M.F., Davison, B.H., Dixon, R.A., Gilna, P., Keller, M., Langan, P., Naskar, A.K., Saddler, J.N., Tschaplinski, T.J., Tuskan, G.A., Wyman, C.E. 2014. Lignin valorization: improving lignin processing in the biorefinery. *Science*, **344**(6185), 1246843.
24. Schutyser, W., Kruger, J.S., Robinson, A.M., Katahira, R., Brandner, D.G., Cleveland, N.S., Mittal, A., Peterson, D.J., Meilan, R., Román-Leshkov, Y., Beckham, G.T. 2018. Revisiting alkaline aerobic lignin oxidation. *Green Chemistry*, **20**(16), 3828-3844.
25. Shikinaka, K., Hashimoto, Y., Kajita, S., Masai, E., Katayama, Y., Nakamura, M., Otsuka, Y., Ohara, S., Shigehara, K. 2013. Thermoplastic Polyesters of 2-Pyrone-4,6-Dicarboxylic Acid (PDC) Obtained

437 from a Metabolic Intermediate of Lignin. *Sen'i Gakkaishi*, **69**(2), 39-47.
438 26. Shikinaka, K., Otsuka, Y., Nakamura, M., Masai, E., Katayama, Y. 2018. Utilization of Lignocellulosic
439 Biomass via Novel Sustainable Process. *J Oleo Sci*, **67**(9), 1059-1070.
440 27. Sonoki, T., Takahashi, K., Sugita, H., Hatamura, M., Azuma, Y., Sato, T., Suzuki, S., Kamimura, N., Masai,
441 E. 2018. Glucose-Free cis,cis-Muconic Acid Production via New Metabolic Designs Corresponding to
442 the Heterogeneity of Lignin. *ACS Sustainable Chemistry & Engineering*, **6**(1), 1256-1264.
443 28. Suzuki, Y., Okamura-Abe, Y., Nakamura, M., Otsuka, Y., Araki, T., Otsuka, H., Navarro, R.R., Kamimura,
444 N., Masai, E., Katayama, Y. 2020. Development of the production of 2-pyrone-4,6-dicarboxylic acid
445 from lignin extracts, which are industrially formed as by-products, as raw materials. *J Biosci Bioeng*.,
446 130(1), 71-75
447 29. Suzuki, Y., Okamura-Abe, Y., Otsuka, Y., Araki, T., Nojiri, M., Kamimura, N., Masai, E., Nakamura, M.
448 2022. Integrated process development for grass biomass utilization through enzymatic saccharification
449 and upgrading hydroxycinnamic acids via microbial funneling. *Bioresour Technol*, **363**, 127836.
450 30. Suzuki, Y., Otsuka, Y., Araki, T., Kamimura, N., Masai, E., Nakamura, M., Katayama, Y. 2021. Lignin
451 valorization through efficient microbial production of beta-ketoadipate from industrial black liquor.
452 *Bioresour Technol*, **337**, 125489.
453 31. Tsuge, Y., Kato, N., Yamamoto, S., Suda, M., Jojima, T., Inui, M.A.-O. 2019. Metabolic engineering of
454 Corynebacterium glutamicum for hyperproduction of polymer-grade L- and D-lactic acid. Appl
455 Microbiol Biotechnol., **103**, 3381-3391.
456 32. Weiland, F., Kohlstedt, M., Wittmann, C. 2022. Guiding stars to the field of dreams: Metabolically
457 engineered pathways and microbial platforms for a sustainable lignin-based industry. *Metab Eng*, **71**,
458 13-41.
459 33. Qian, Y., Otsuka, Y., Sonoki, T., Mukhopadhyay, B., Nakamura, M., Masai, E., Katayama, Y., Okamura-
460 Abe, Y., Jellison, J., Goodell, B. 2016. Engineered Microbial Production of 2-Pyrone-4,6- Dicarboxylic
461 Acid from Lignin Residues for Use as an Industrial Platform Chemical. *BioResources*, **11**(3), 6097-
462 6109.

463

464 **Figure captions**

465 **Figure 1.** PDC production in fed-batch fermentation using Na-medium I. (A) Artificial metabolic
466 pathways of *P. putida* PpY1100 to produce PDC from VA. Abbreviations: VA, vanillic acid; PCA,
467 protocatechuic acid; CHMS, 4-carboxy-2-hydroxymuconate-6-semialdehyde; PDC, 2-pyrone-4,6-
468 dicarboxyric acid. Enzymes: VanAB, VA *O*-demethylase; LigAB, PCA 4,5-dioxygenase; LigC,
469 CHMS dehydrogenase. (B) Glucose (Glc) was added stepwise as a growth source. (C) Glc was
470 added continuously as a growth source. Two independent experiments are indicated with solid and
471 dashed lines. P1-P6 (Blue arrows) indicate sampling points for metabolomic analysis.

472

Figure 2. Metabolomic analysis in Na-medium I with the stepwise addition of Glc.

The concentration of each component is depicted in the heat map (blue: low, red: high). P1–P6 correspond to Fig. 2A. P1: initial-term of cell growth, P2: mid-term of cell growth, P3: before the addition of Glc, P4: initial-term of PDC production after initiating Glc and VA feed, P5: late-term of PDC production, P6: after VA accumulation.

Figure 3. Metabolomic analysis in Na-medium I with the continuous addition of Glc.

The concentration of each component is shown in the heat map (blue: low, red: high). P1–P6 correspond to Fig. 2B. P1: initial-term of cell growth, P2: mid-term of cell growth, P3: initial-term of PDC production after Glc and VA feed, P4: mid-term of PDC production, P5: late-term of PDC production, P6: the end of fermentation.

Figure 4. PDC production in fed-batch fermentation using Na-medium II. The red arrow indicates the feeding point of VA.

Figure 5. Comparison of PDC extraction processes under different culture conditions using sodium and ammonium salts.

Figure 6. PDC production in fed-batch fermentation using NH_3-medium. The red arrow indicates the feeding point of VA.

Figure

Click here to access/download;Figure;Figures_R1.pptx

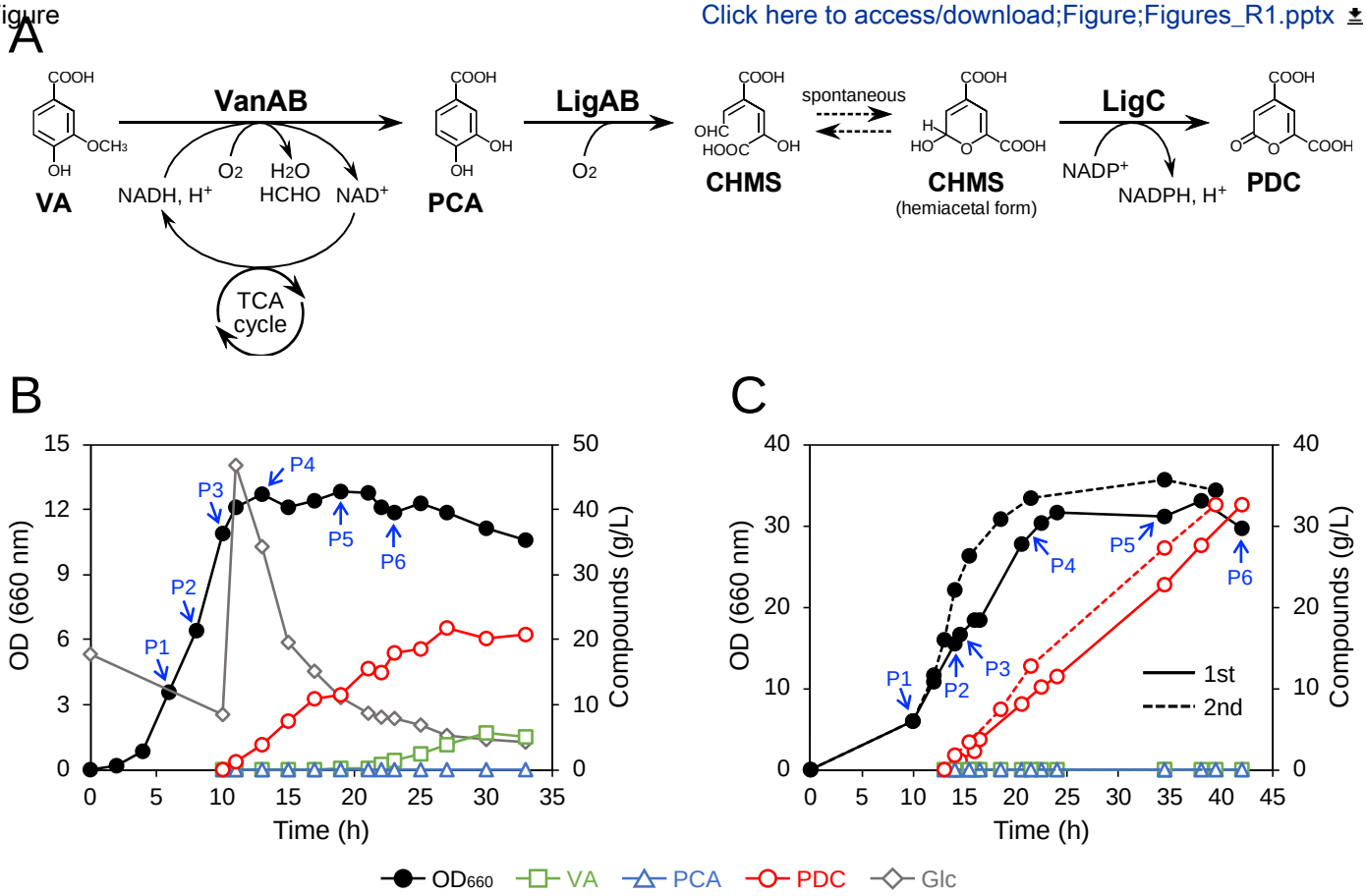

Figure 1, Otsuka et al.

		Concentration (pmol/OD・mL)					
	Compounds	P1	P2	P3	P4	P5	P6
Amino acids	Gly	26.2	18.25	36.65	290.65	33.95	35.7
	Ala	44.55	40	84.6	133.5	23.85	27.05
	Ser	27.3	22.4	28.6	425.55	20.95	19.4
	Pro	7.8	6.35	14	36.25	4.4	9.65
	Val	15.25	11.75	29.15	64.95	14.75	17
	Thr	12.95	11.25	23.15	84.35	6.4	18.4
	Ile	2.95	3.4	6.6	39.5	2.8	3.8
	Leu	3.9	5.35	12.05	52.4	5.45	6.4
	Asn	1.05	0.7	0.85	26.35	0.485	0.5
	Asp	31.65	25.75	83.6	99.25	12.4	17.6
	Gln	7.05	5.65	19.5	4.9	19.5	89.3
	Lys	107.5	92.4	71.55	116.15	28.7	15
	Glu	164.95	125.15	538.35	107.45	117.55	230.4
	Met	3.35	4.35	9.1	7.8	3	3.05
	His	4.45	5	8.45	51	3.2	6.15
	Phe	2.9	5.6	12.1	32.5	3.05	3.9
	Arg	5	21.85	12.05	27.95	3.7	1.8
	Tyr	7.35	6.85	13	41.5	3.15	6.55
	Trp	2.45	2.3	4.95	8.6	2.25	2.6
Energy carriers	NAD	262.35	177.65	260.5	23.2	65.85	55.5
	NADP	95.35	80.7	91.9	18.85	31.55	18.1
	ATP	74.55	49.3	73.4	8.25	12.65	26.4
	ADP	137.3	102.4	107.7	25.05	34.8	30.65
Glycolysis	Glucose 6-phosphate	23.7	19.6	48.2	18.75	19.35	18.65
	Fructose 6-phosphate	15.1	14.65	27.4	13.7	9.1	6.85
	Fructose 1,6-diphosphate	5.4	7.85	8.05	5	3.05	1.3
	Dihydroxyacetone phosphate	8.6	6.85	14.6	11.55	7	2.05
	3-Phosphoglyceric acid	17.2	26.15	70.3	32.25	0	0
	2-Phosphoglyceric acid	3.25	3.1	8.8	2.1	3	2.05
	Phosphoenolpyruvic acid	5.75	5.4	16.1	3.95	8	8.35
	Pyruvic acid	0	0	16.75	54.2	10.75	0
	6-Phosphogluconic acid	1	0.75	1.75	1.55	1.75	0.9
	Ribulose 5-phosphate	4.4	3.9	7.35	4.8	3.5	1.5
	Ribose 5-phosphate	10.4	6.4	7.95	3.15	2.95	1.75
	Sedoheptulose 7-phosphate	34.45	31.95	48.2	8.05	8.55	7.55
	Erythrose 4-phosphate	2.1	1.95	2	0	0	0
TCA cycle	Acetyl CoA_divalent	23.3	12.8	25.65	2.4	5.3	1.1
	Citric acid	11.85	6.6	24.5	11.9	23.8	13.65
	Isocitric acid	1.25	0	1.35	0	1.75	0
	2-Oxoglutaric acid	0	0	5.05	102.15	315.6	92.65
	Succinic acid	21.35	19.6	30.25	58.25	149.15	93.55
	Fumaric acid	0	0	3.95	0	2.6	2.5
	Malic acid	7.75	4.85	2.85	4.2	4.05	3.3

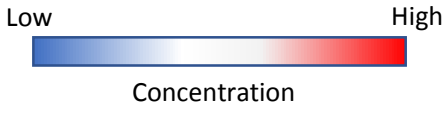

Figure 2, Otsuka et al.

	Compounds	Concentration (pmol/OD・mL) P1	P2	P3	P4	P5	P6
Amino acids	Gly	29	55	95	61	43	24
	Ala	153	119	186	127	40	32
	Ser	25	41	63	37	10	7.8
	Pro	24	18	27	17	2.7	2.3
	Val	28	39	72	39	11	10
	Thr	46	61	78	34	7.2	6.1
	Ile	6.5	7.2	15	11	4.8	5
	Leu	7.4	16	32	21	11	12
	Asn	0.8	0.6	0	0	0	0
	Asp	97	70	68	32	38	7.9
	Gln	39	46	15	8.6	3.6	1.4
	Lys	73	86	113	56	18	16
	Glu	1103	629	464	287	873	85
	Met	11	17	22	10	2.6	2.2
	His	20	25	33	15	3.5	3.5
	Phe	17	32	48	21	5	4.1
	Arg	5.9	15	18	3.2	1	0.9
	Tyr	21	24	31	15	9	5.5
	Trp	9.3	11	12	5.9	2	3.3
Energy carriers	NAD	533	620	505	191	52	25
	NADP	202	204	182	101	33	15
	ATP	188	145	138	46	14	8.2
	ADP	241	243	197	81	32	22
Glycolysis	Glucose 6-phosphate	63	34	16	9	5.2	2.8
	Fructose 6-phosphate	55	14	6.6	5.3	3	1.3
	Fructose 1,6-diphosphate	13	7.1	3.4	1	0	0
	Dihydroxyacetone phosphate	24	4.1	2.7	2.1	1.7	0
	3-Phosphoglyceric acid	79	137	73	37	17	16
	2-Phosphoglyceric acid	13	23	20	8.2	8.3	1.3
	Phosphoenolpyruvic acid	35	50	49	24	10	5.7
	Pyruvic acid	0	0	0	0	0	0
	6-Phosphogluconic acid	3.9	3.6	1.3	1.6	0.6	0.7
	Ribulose 5-phosphate	10	2.7	0	0	2.8	0
	Ribose 5-phosphate	29	8.9	5.8	3.6	2	1.2
	Sedoheptulose 7-phosphate	88	27	12	7.2	4.5	2.4
	Erythrose 4-phosphate	3.1	0	0	0	0	0
TCA cycle	Acetyl CoA_divalent	48	39	30	22	8.1	6.6
	Citric acid	20	20	13	11	7.5	5.2
	Isocitric acid	0	0	0	0	0	0
	2-Oxoglutaric acid	4	6.1	4.4	0	3.9	0
	Succinic acid	24	26	14	16	6.8	7.9
	Fumaric acid	0	0	0	0	0	0
	Malic acid	3.3	5.1	5.8	6.9	7.4	7.1

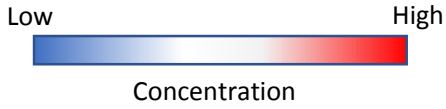

Figure 3, Otsuka et al.

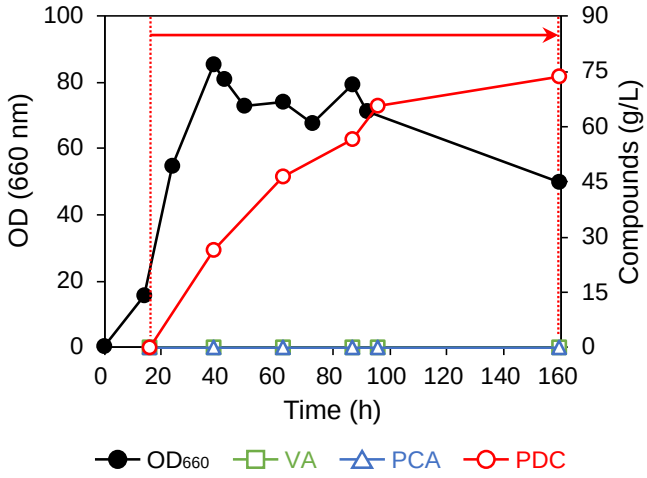

Figure 4, Otsuka et al.

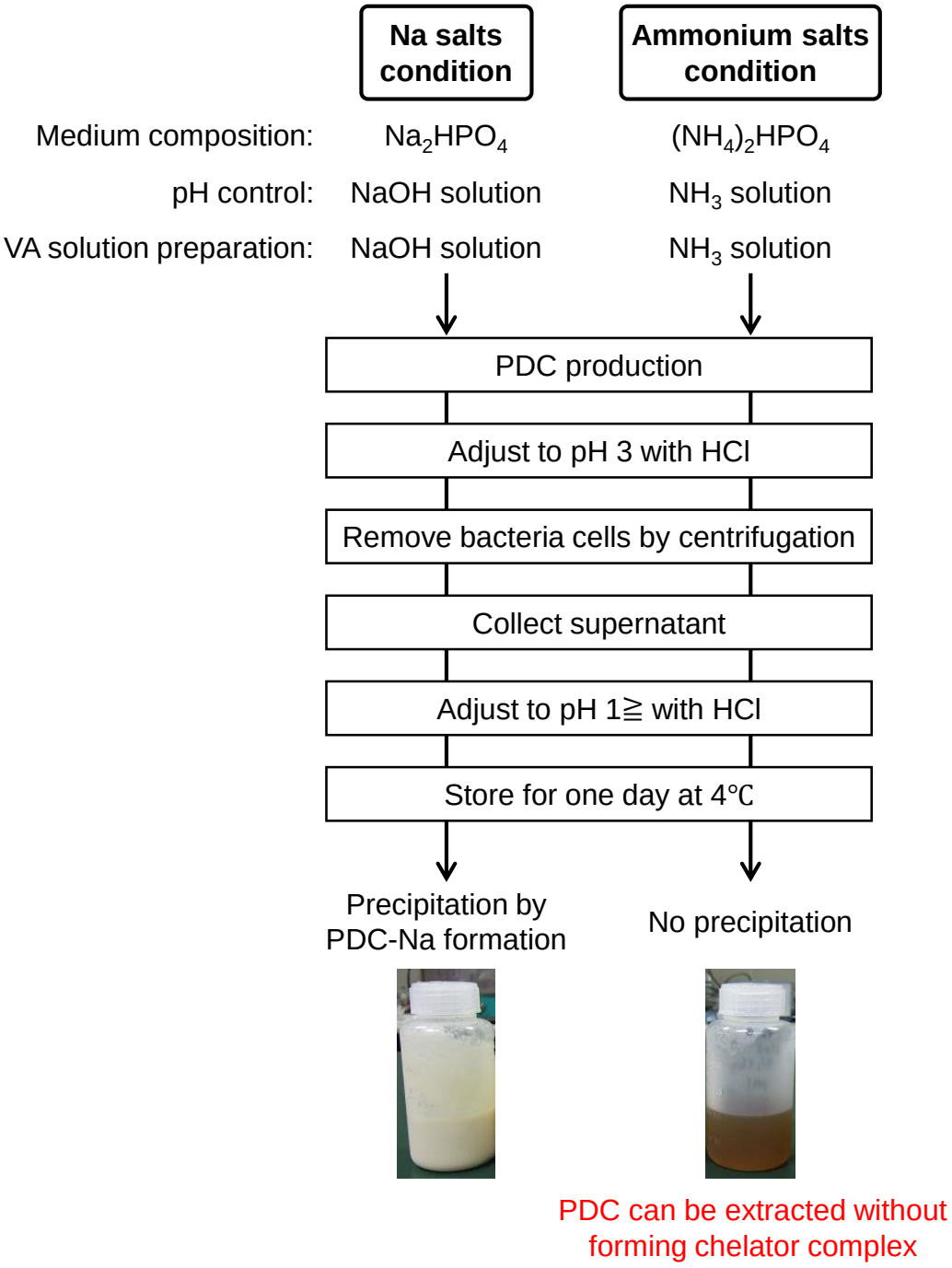

Figure 5, Otsuka et al.

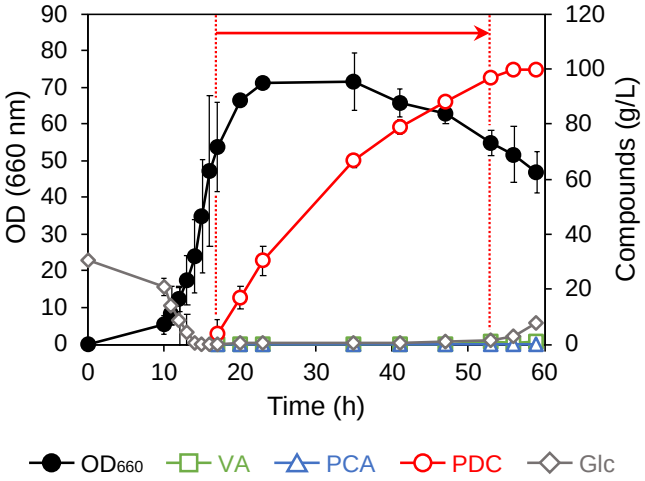

Figure 6, Otsuka et al.

Declaration of interests

☒The authors declare that they have no known competing financial interests or personal relationships that could have appeared to influence the work reported in this paper.

☐The authors declare the following financial interests/personal relationships which may be considered as potential competing interests:

CRediT authorship contribution statement

Yuichiro Otsuka: Methodology, Validation, Investigation, Formal analysis, Writing – original draft, Writing – review & editing, Visualization, Supervision, Project administration, Funding acquisition. **Takuma Araki:** Methodology, Validation, Investigation, Resources, Writing – review & editing, Visualization. **Yuzo Suzuki:** Methodology, Investigation, Resources, Writing – review & editing. **Masaya Nakamura:** Methodology, Investigation, Writing – review & editing. **Naofumi Kamimura:** Resources, Investigation, Writing – review & editing. **Eiji Masai:** Resources, Investigation, Writing – review & editing.